Optimizing Resource and Restauration Scheduling for Power Distribution Systems After a Natural Hazards: A Case Study with Volcanic Lahars

Llumigusín Cachipuz, Grace Alexandra y Yánez Chancusig, Jhonatan Alexander

Departamento de Eléctrica y Electrónica

Carrera de Ingeniería en Electromecánica

Artículo académico, previo a la obtención del título de Ingeniera en Electromecánica

Ing. Ortiz Villalba, Diego Edmundo MSc.

16 de febrero del 2022

Optimizing Resource and Restoration Scheduling for Power Distribution Systems After a Natural Hazard: A Case Study with Volcanic Lahars

G. Llumigusín-Cachipuz, J. Yánez-Chancusig, D. Ortiz-Villalba, *Member, IEEE*,
M. Saltos-Rodríguez, *Student Member, IEEE*, and A. Velásquez-Lozano, *Student Member, IEEE*
Universidad de las Fuerzas Armadas ESPE
Sangolquí-Ecuador
[gallumigusin, jaynezc, ddortiz5, masaltos2, amvelasquez1]@espe.edu.ec

***Abstract*—High impact low probability events (HILP) such as natural hazards significantly affect the infrastructure of power distribution systems (PDS) leading to considerable social and economic loss. This paper presents a novel methodology for optimizing resource and restoration scheduling in PDS after a natural hazards focusing on reducing operational costs during PDS recovery. The proposed methodology includes a mixed integer linear programming optimization problem in which a DC optimal power flow model is solved. The proposed methodology was evaluated in the IEEE 34-node test feeder and in a real-world case in two PDS: the San Rafael and Salcedo feeders in Cotopaxi-Ecuador. The results show the effectiveness of the proposed methodology compared with traditional recovery criteria.**

***Index Terms*—power distribution systems, volcanic eruption, DC optimal power flow, system recovery, resources optimization.**

I. Introduction

High impact low probability events (HILP), such as hurricanes, earthquakes, volcanic eruptions, among others, can seriously affect power distribution systems (PDS). There are statistical records of important destructive events, such as in the United States, which records 78% of all its interruptions in the power distribution systems caused by natural disasters [1]. In the particular case of a volcanic eruption, the Irazú volcano erupted in 1963, affecting a large part of the population of Costa Rica, in which infrastructure and essential services were damaged, reaching an estimated loss 601.5 million USD [2]. In recent days, the eruption of the La Palma volcano has demonstrated the devastation that might occur when a volcano erupts. La Palma, located on one of the smallest and western-most Canary Islands in Spain, caused more than 6,000 people to be evacuated and an estimated damage exceeding 466 million USD. In this context, and others where climate change hazards are multiplying, planning for the effects of these hazards is becoming ever more critical. Power system resilience is defined as the resistance and restoration capacity of the electrical networks to HILP events affecting its integrity [3]. The hazard conditions caused by HILP events require power distribution companies to plan restoration and operation in scenarios in which HILP events can occur. However, there are a limited number of studies that address the optimized restoration of resilient PDS against natural hazards. For instance, in [4] the system is restored using distributed generators and the reconfiguration of the system; this methodology is intended for power network damage due to extreme weather events. The authors in [5], present an optimized strategy for the location of reclosers for fault isolation and service restoration. In [6] a fuzzy approach is implemented to improve system restoration, which takes into account the priority of loads and the distance between depots and faults in an effort to avoid using only expert criteria in the restoration of the PDS.

To avoid decision-making based on traditional methods that do not consider critical loads, the available resources, and the energy not supplied (ENS), our paper presents a novel methodological framework for optimal resource and restoration scheduling in PDS operation subsequent to HILP events. The main contributions of this work are as follows: i) A DC-Optimal Power Flow (DC-OPF) model implemented under contingencies that can optimize system restoration, quantifying the ENS of the PDS caused by the damages in the electrical infrastructure from an HILP event. ii) A strategy to optimize mobilization of crews and mobile generators to recover and supply energy to the PDS considering ENS, arrival time at depot and nodes, and critical loads. iii) A Real-World application of the method in two PDS: San Rafael and Salcedo feeders in Cotopaxi (Ecuador), considering the impact of lahar occurrence after an eruption of the Cotopaxi volcano.

II. Methodology

The proposed methodological framework is presented in Fig. 1, which comprises three general stages described below.

A. Input data

The contingency scenario uses real-time post-event data, and the proposed methodology is applied. Moreover, our proposal can be applied to historical contingency scenarios, in which vulnerability curves can be used to assess the impact of HILP events.

The PDS is represented as a set of nodes (Ω_B) and power distribution lines (Ω_L) with their electric technical characteristics and electrical infrastructure georeferenced data. In addition, the depot is georeferenced to identify the distances between nodes and depots located within the concession area

of the distribution company. Finally, the available resources of the distribution company for any contingency scenario are considered.

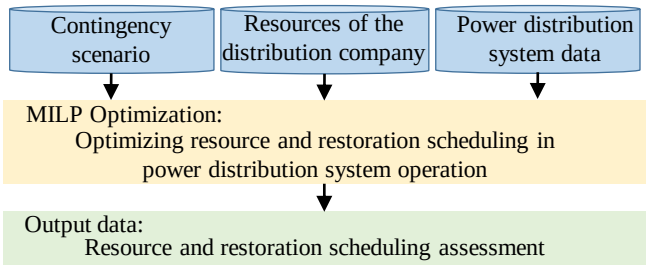

Fig. 1. Proposed methodology to optimizing resource and restoration scheduling in power distribution system operation

B. MILP Optimization Problem

Once the contingency scenarios have been defined, a mixed-integer linear programming (MILP) optimization is formulated resolving a DC-OPF model. The unavailability matrices of a contingency scenario of nodes $(\psi_{i,t})$, and distribution lines $(\gamma_{ij,t})$ are included. The objective function minimizes the operating cost of the PDS during system restoration time. The MILP optimization is solved using FICO XPRESS 8.8.0 software [7]. The problem formulation is detailed in Section III.

C. Output data

The results obtained are evaluated using resilience metrics. ENS is used as a reliability metric for system resilience analysis. It is also possible to quantify additional metrics such as the energy index of unreliability (EIU), which indicates the relationship between ENS and energy demand during the restoration time estimation [8]. Moreover, the $\Phi\Lambda E\Pi$ resilience metrics can be applied to measure the performance of the different phases that a power system might experience during an extreme event [9]. In this case, the Π-metric has been chosen to quantify how fast the operational and infrastructure resilience recover after the HILP event occurs.

III. Formulation Problem

A. Objective Function

The objective function (OF) of MILP optimization is presented in (1), which minimizes the operational costs (OC). The OF considers the cost of the ENS (OC_{ENS}), the cost of mobile generating units (OC_{MG}) and the cost of the resource mobilization ($OC_{Resource}$) of the electrical company (including crews and mobile generating units). Equation (2) represents the cost of ENS during the time horizon of evaluation (T). The cost of ENS varies according to the load priority on the nodes of the PDS (N_B). Equation (3) indicates the operating costs of the mobile generating units (N_{MG}), in which fuel costs (C^{fuel}) and the cost of CO_2 emissions (C^{CO_2}) are considered. To simplify the model, the linearization of fuel consumption by mobile generating units ($f_{i,t}^{fuel}$) is not considered. $E_{i,t}^{CO_2}$ represents the total emission of CO_2 due to the use of mobile generating units. Equation (4) considers the resource mobilization cost C^{RM} of the distribution company (N_R) such as crews and mobile generating units, where $\lambda_{i,w,t}$ and $\tau_{i,w,t}$ correspond to the binary variables that indicate the arrival and departure of resources to the node, respectively. The continuous optimization variable d_i indicates the distances between depot and nodes. Finally, equation (5) represents whether the routes from the depots to nodes are available through the binary parameter σ_i. The Big M method is used to decouple the arrival times for mobile generating units.

$$Min\ OF = OC_{ENS} + OC_{MG} + OC_{Resource} \tag{1}$$

$$OC_{ENS} = \sum_{i=1}^{N_B}\sum_{t=1}^{T} C_i^{ENS} ENS_{i,t} \tag{2}$$

$$OC_{MG} = \sum_{i=1}^{N_{MG}} [C^{fuel} f_{i,t}^{fuel} + C^{CO_2} E_{i,t}^{CO_2}] \tag{3}$$

$$OC_{Resource} = \sum_{i=1}^{N_B}\sum_{w=1}^{N_R}\sum_{t=1}^{T} C^{RM}(\lambda_{i,w,t} + \tau_{i,w,t}) d_i \tag{4}$$

$$d_i = D_i + (1-\sigma_i)M \qquad i \in \Omega_B \tag{5}$$

B. Resource Mobilization

The mobile generating units and crews are considered as resources of the distribution company (Ω_R) that will be used to supply the demand and recover the PDS, respectively, after the HILP event occurs. This set of optimization problem constraints focuses on determining each departure and arrival of the resources from the depots to the nodes considering displacement times to establish optimal resource and restoration scheduling during the evaluation horizon. Constraints (6) and (7) impose that $\lambda_{i,w,t}$ and $\tau_{i,w,t}$ take the appropriate values when a resource arrives to or departs from a node. $\chi_{i,w,t}$ is a binary variable that represents the state of the resource in the node i. Likewise, the constraints (8) and (9) ensure that the resource arrival to $(\vartheta_{i,w,t})$ and departure from $(\rho_{i,w,t})$ the depot take the appropriate values. $\nu_{w,t}$ is a binary variable that represents the state of resources in the depot. Constraint (10) represents that the resource w cannot be at the node or in the depot simultaneously t.

$$\lambda_{i,w,t} - \tau_{i,w,t} = \chi_{i,w,t} - \chi_{i,w,t-1} \qquad i \in \Omega_B; w \in \Omega_R \tag{6}$$

$$\lambda_{i,w,t} + \tau_{i,w,t} \leq 1 \qquad i \in \Omega_B; w \in \Omega_R \tag{7}$$

$$\sum_{i=1}^{N_B}[\vartheta_{i,w,t} - \rho_{i,w,t}] = \nu_{w,t} - \nu_{w,t-1} \qquad i \in \Omega_B; w \in \Omega_R \tag{8}$$

$$\sum_{i=1}^{N_B}[\vartheta_{i,w,t} + \rho_{i,w,t}] \leq 1 \qquad i \in \Omega_B; w \in \Omega_R \tag{9}$$

$$\chi_{i,w,t} + \nu_{w,t} \leq 1 \qquad i \in \Omega_B; w \in \Omega_R \tag{10}$$

Constraint (11) ensures the arrival time from the depots to the node in the initial hours. The constraints (12) and (13) are required to ensure the arrival and departure time of resources from the depot to the node, or vice versa. These conditions are represented by T_i^{RM}. Equations (14) and (15) guarantee the final arrival and departure times of the resources from the depot to the node or from the node to the depot, respectively.

$$\sum_{t=1}^{T_i^{RM}} \lambda_{i,w,t} = 0 \qquad i \in \Omega_B; w \in \Omega_R \tag{11}$$

$$\rho_{i,w,t} = \lambda_{i,w,t+T_i^{RM}-1} \qquad i \in \Omega_B; w \in \Omega_R \tag{12}$$

$$\forall t = 1, ..., |T| - T_i^{RM} + 1 \geq 1$$

$$\tau_{i,w,t} = \vartheta_{i,w,t+T_i^{RM}-1} \quad i \in \Omega_B; w \in \Omega_R \quad (13)$$
$$\forall t = 1, ..., |T| - T_i^{RM} + 1 \geq 1$$
$$\sum_{k=t}^{T}(1 - \lambda_{i,w,k} - \rho_{i,w,t}) \geq 0 \quad i \in \Omega_B; w \in \Omega_R \quad (14)$$
$$1 \leq \forall t = T - T_i^{RM} + 1, ..., |T| \leq T$$
$$\sum_{k=t}^{T}(1 - \vartheta_{i,w,k} - \tau_{i,w,t}) \geq 0 \quad i \in \Omega_B; w \in \Omega_R \quad (15)$$
$$1 \leq \forall t = T - T_i^{RM} + 1, ..., |T| \leq T$$

Constraints (16) and (17) represent the time T_w^D during which the resources remain in the depot for refueling and checking technical conditions. The constraints (18) and (19) represent the recovery time of the nodes T_i^R.

$$\sum_{k=t}^{t+T_w^D-1} \nu_{w,k} \geq T_w^D \sum_{i=1}^{N_B} \vartheta_{i,w,t} \quad i \in \Omega_B; w \in \Omega_R \quad (16)$$
$$\forall t = 1, ..., |T| - T_w^D + 1 \geq 1$$
$$\sum_{k=t}^{T_w^D}(\nu_{w,k} - \sum_{i=1}^{N_B} \vartheta_{i,w,t}) \geq 0 \quad i \in \Omega_B; w \in \Omega_R \quad (17)$$
$$1 \leq \forall t = T - T_w^D + 1, ..., |T| \leq T$$
$$\sum_{k=t}^{t+T_i^R-1} \chi_{i,w,k} \geq T_i^R \lambda_{i,w,t} \quad i \in \Omega_B; w \in \Omega_R \quad (18)$$
$$\forall t = 1, ..., |T| - T_i^R + 1 \geq 1$$
$$\sum_{k=t}^{T_i^R}(\chi_{i,w,k} - \sum_{i=1}^{N_B} \lambda_{i,w,t}) \geq 0 \quad i \in \Omega_B; w \in \Omega_R \quad (19)$$
$$1 \leq \forall t = T - T_i^R + 1, ..., |T| \leq T$$

C. Nodes and lines restoration

Constraints (20) and (21) are used to determine the nodes that are considered repaired when the crew departs the node. In this context, constraint (20) restricts the affected node to be repaired by only one crew. Constraint (21) indicates that the restored component becomes available after it is repaired and remains available in all subsequent time evaluation horizons. For instance, if $\tau_{i,w,t} = [0, 0, 1, 0, 0, 0]$ then $\psi_{i,t} = [0, 0, 1, 1, 1, 1]$ [10].

$$\sum_{w=1}^{N_R} \tau_{i,w,t} \leq 1 \quad i \in \Omega_B \quad (20)$$
$$\psi_{i,t} = \sum_{k=1}^{t...|T|} \sum_{w=1}^{N_R} \tau_{i,w,k} \quad i \in \Omega_B \quad (21)$$

For the recovery of distribution lines, the line ij is assumed to be available if the nodes i and j associated with the line are also available. This is represented by the set of constraints (22)-(24), in which the product of binary variables of node availability is carried out.

$$\gamma_{ij,t} \leq \psi_{i,t} \quad i \neq j \in \Omega_B, ij \in \Omega_L \quad (22)$$
$$\gamma_{ij,t} \leq \psi_{j,t} \quad i \neq j \in \Omega_B, ij \in \Omega_L \quad (23)$$
$$\gamma_{ij,t} \geq \psi_{i,t} + \psi_{j,t} - 1 \quad i \neq j \in \Omega_B, ij \in \Omega_L \quad (24)$$

D. Thermal generating unit constraints

The thermal generation model presented in [11] is implemented in this paper to model mobile generating units. Equation (25) corresponds to natural gas consumption $f_{i,t}^{fuel}$, where $P_{i,t}^{MG}$ is the output power from a mobile generating unit, u^{MG} is the energy density of the natural gas consumed in kWh/kg, and η^{MG} is power efficiency. Equation (26) represents the CO_2 (E^{CO_2}) that depends on the carbon footprint for the energy produced (K^{CO_2}). Finally, constraint (27) imposes bounds on the mobile generating units and considers the state of the mobile generator ($\chi_{i,w,t}$) in the node.

$$f_{i,t}^{fuel} = \frac{P_{i,t}^{MG}}{u^{MG}\eta^{MG}} \quad i \in \Omega_B \quad (25)$$
$$E_{i,t}^{CO_2} = K^{CO_2} u^{MG} f_{i,t}^{fuel} \quad i \in \Omega_B \quad (26)$$
$$0 \leq P_{i,t}^{MG} \leq \sum_{w=1}^{N_{MG}} P_w^{MG,max} \chi_{i,w,t} \quad i \in \Omega_B \quad (27)$$

E. DC optimal power flow

The DC model presented in [12] is implemented in our work to perform the PDS operation. Constraint (28) ensures the generation-demand balance at each node of the system. Constraint (29) defines that the ENS should not exceed the connected demand at each bus to correctly quantify the ENS in each bus. Equation (30) represents the constraint related to the capacity limits of the transmission lines. Finally, equation (31) models Kirchhoff's second law based on the Big M disjunctive technique, where M is a sufficiently large positive constant, which decouples the voltage angles of the busbars associated with the lines that are disconnected due to a contingency in the system.

$$P_{i,t}^{Grid} + P_{i,t}^{MG} + \sum_{ij \in \Omega_{LT}} P_{ij,t}^{line} + ENS_{i,t} = D_i \quad i \in \Omega_B \quad (28)$$
$$0 \leq ENS_{i,t} \leq D_i \quad i \in \Omega_B \quad (29)$$
$$-\gamma_{ij,t} P_{line}^{max} \leq P_{ij,t}^{line} \leq P_{line}^{max} \gamma_{ij,t} \quad ij \in \Omega_L \quad (30)$$
$$-M(1 - \gamma_{ij,t}) + \frac{\delta_{i,j} - \delta_{j,t}}{x_{ij}} \leq P_{ij,t}^{line} \leq \frac{\delta_{i,t} - \delta_{j,t}}{x_{ij}} + M(1 - \gamma_{ij,t}) \quad i \neq j \in \Omega_B, ij \in \Omega_L \quad (31)$$

IV. Case Study and Results

To evaluate the efficiency of the proposed methodology, it was applied in the IEEE 34-node test feeder and in two PDS: San Rafael and Salcedo feeders in Cotopaxi, Ecuador. In both PDS, the occurrence of lahars and their impact are modelled. ENS costs are established for the load types depending on their priority level. In addition, our proposed optimal model is compared with the expert criteria model in which the recovery nodes nearer the depot are recovered to reconnect to the main grid.

A. IEEE 34-node test feeder

1) System: The IEEE 34-node test feeder presented in [13], is composed of 33 branches and node loads. The loads are characterized using representative residential, commercial, and industrial daily load curves obtained from [14]. It is assumed that the resources available are two crews and two mobile generating units with a rated capacity of 100 and 500 kW. Finally, node repair time is defined as five hours.

2) Lahar event: Fig. 2 shows the illustrative case. The PDS is assumed to be affected by volcanic lahars and impacts nodes 7, 15 and 23, forming four islanding systems.

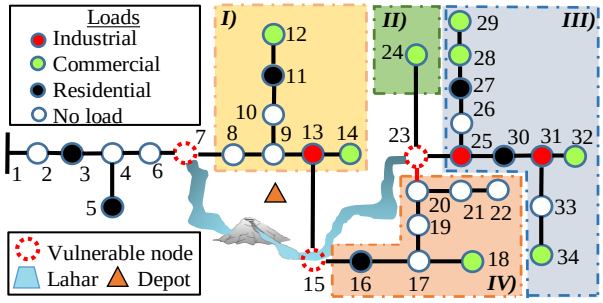

Fig. 2. IEEE 34-node test feeder and nodes unavailable after HILP event occurs

3) Results: The results show that operational costs are reduced from 9,349 USD to 8,880 USD when our proposed optimal model is applied. The results of resource scheduling applied to the IEEE 34-node test feeder are shown in Table I. The mobile generating unit (G1 and G2) scheduling considering both approaches is carried out in the same way. However, the crew scheduling (C1 and C2) is carried out differently. For the expert criteria model, the recovery of nodes 7, 15 and 25 is carried out sequentially because the island systems formed are reconnected to the main grid depending on how the system is recovering. For the optimal model, the sequence of node recovery is 7-25-15. This configuration allows faster system recovery compared to applying expert criteria. Fig. 3 shows the system recovery. The results show that applying the optimal model the system recovers 3 hours faster than with the expert criteria model.

TABLE I
RESULTS OF RESOURCE SCHEDULING TO THE IEEE-34 NODE TEST FEEDER

Case	G1		G2		C1		C2	
	Node	Time	Node	Time	Node	Time	Node	Time
Optimal	13	3-11	25	3-48	7	2-11	23	6-15
	25	15-48	-	-	15	15-24	-	-
Expert	13	3-11	25	3-48	7	2-11	15	4-13
	25	15-48	-	-	23	18-27	-	-

Table II shows the resilience metric obtained from IEEE 34-node test feeder after the HILP event occurs. These metric are divided into three groups to visualize how the system is affected by energy supply capacity, operation and infrastructure. Results show the energy supply capacity taking into account the ENS during the time evaluation horizon applying the optimal model is reduced by 0.2 MWh as compared with the expert criteria model. On the other hand, the EIU for industrial (EIU_I) and commercial (EIU_C) loads is reduced by 2.95% and 3%, respectively, while for residential loads (EIU_R) does not change. Furthermore, the Π resilience metric indicates that our proposed optimal model recovered the PDS faster than the expert criteria model in terms of operational and infrastructure resilience.

B. San Rafael and Salcedo feeders

1) System: The data required to model the PDS was obtained from the geoportal of the ELEPCO utility available

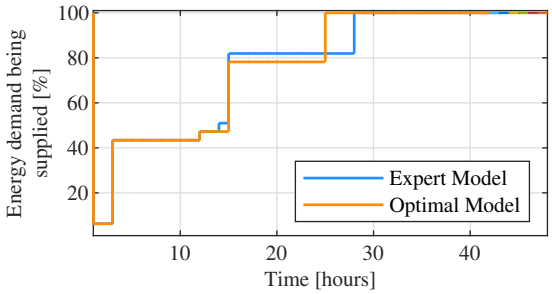

Fig. 3. Evolution of the recovery of unsupplied energy applied to IEEE 34-node test feeder

TABLE II
IEEE 34-NODE TEST FEEDER RESILIENCE METRIC RESULTS

Case	ENS [MWh]	EIU_I [%]	EIU_C [%]	EIU_R [%]	*Operational resilience* Π-loads [kW/h]	*Infrastructure resilience* Π-nodes [Nodes/h]
Optimal	17.34	14.56	23	34.5	6.05	0,12
Expert	17.54	17.51	26	34.5	5.41	0.11

at [15]. The feeders are represented with 71 electrical nodes. Priority loads (hospitals, health centre, emergency shelters, industries) were defined according to the Cotopaxi volcano hazard map published in [16]. The resource depot is identified in the system as shown in Fig. 4, in which there is a mobile generator with rated power of 5 MW and five crews for system recovery. In addition, the time evaluation horizon is fixed at 144 hours.

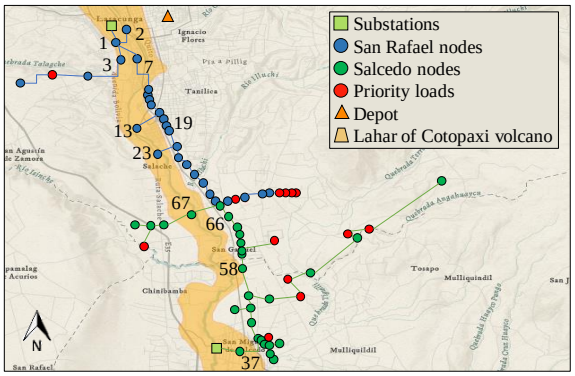

Fig. 4. San Rafael and Salcedo feeders one-line diagram considering lahar impacts and critical loads.

2) Lahar event: The data of lahars that occurred in 1877 during the Cotopaxi volcano eruption was used [17] to define the contingency scenarios. The one-line diagram of the San Rafael and Salcedo PDSs and the lahar formed by the Cotopaxi volcano eruption are shown in Fig. 4.

TABLE III
RESULTS OF RESOURCE SCHEDULING TO THE SAN RAFAEL AND SALCEDO-FEEDERS

	Optimal		*Expert*			*Optimal*		*Expert*	
	Node	Time	Node	Time		Node	Time	Node	Time
G	19	2-144	66	2-144	C3	13	24-53	3	2-53
	-	-	-	-		3	78-129	67	62-77
C1	23	4-59	13	3-18	C4	67	8-23	-	-
	-	-	23	24-80		1	68-129	1	62-53
C2	7	2-129	7	2-129	C5	-	-	2	2-57
	-	-	-	-		2	74-129	58	55-113

3) Results: The results of resource scheduling applied in two PDS — the San Rafael and Salcedo feeders — are shown in Table III. The mobile generating unit (G) is scheduled for both models in the same way. However, it is connected to different nodes in the same islanding system. Likewise, the crews (C1-C5) are scheduled differently for both models. For the expert criteria model, the recovery of nodes is carried out depending on the unavailable nodes nearer to the depot. In the optimal model, the sequence of node recovery can improve system recovery in comparison with the expert criteria, as shown in Fig. 4. The energy demand being supplied is 88% for both approaches at 144 hours. However, the optimal model approach has better performance in the resilience metrics. Table IV shows a recovery improvement at 50% for the optimal model, a higher speed than the expert criteria model with 5.10 kW/h and 1.31 Nodes/h, which significantly reduces the ENS of 73 MWh and saves 23,079 USD in the operational cost. Furthermore, the EIU to priority loads is reduced by 15%.

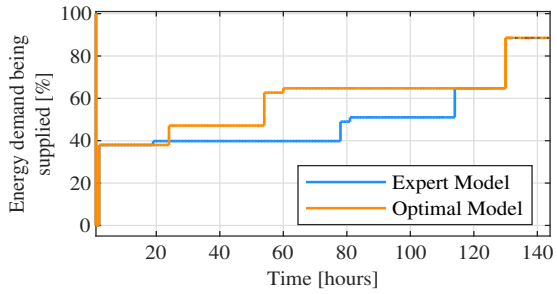

Fig. 5. Evolution of the recovery of unsupplied energy applied to San Rafael and Salcedo feeders

TABLE IV
SAN RAFAEL AND SALCEDO FEEDERS RESILIENCE METRIC RESULTS

Case	ENS [MWh]	EIU_P [%]	*Operational resilience-loads* $\Pi_{50\%}$ [kW/h]	$\Pi_{80\%}$ [kW/h]	*Infrastructure resilience-nodes* $\Pi_{50\%}$ [Nodes/h]	$\Pi_{80\%}$ [Nodes/h]
Optimal	331.55	19	5.10	1.28	1.31	1.10
Expert	404.55	34	3.44	1.28	0.88	1.10

V. CONCLUSIONS

This paper presents a novel methodology for resilience enhancement by optimizing resource and restoration scheduling in power distribution system operations subsequent to an HILP. The proposed methodology includes a mixed-integer linear programming optimization problem in which a DC optimal power flow model is solved. The methodology is applied on the IEEE 34-node test feeder and in two PDS — the San Rafael and Salcedo feeders in Cotopaxi-Ecuador — in which the occurrence of lahars is considered. The results show that the operational cost for the systems under study is reduced when our optimal model is considered compared to recovery using expert criteria. Furthermore, the resilience metrics in terms of energy supply capacity, operational and infrastructure resilience were improved demonstrating that our proposed methodology enhances the resilience of the PDS against natural hazards. We demonstrate the advantage of our proposed methodology through case studies. Then, compared to the expert criteria approach, we demonstrate that our approach with optimized resource and restoration scheduling has better performance in terms of resilience enhancement for PDS operation.

ACKNOWLEDGMENT

The authors would like to thank to “Academic Partner Program” (APP) of FICO Xpress Optimization Suite.

REFERENCES

[1] R. J. Campbell and S. Lowry, “Weather-related power outages and electric system resiliency,” Congressional Research Service, Library of Congress Washington, DC, 2012.
[2] I. Aguilar and G. E. Alvarado, “Pérdidas humanas y económicas causadas por el vulcanismo en costa rica entre 1953 y 2005,” *Revista Geológica de América Central*, no. 51, pp. 93–128, 2014.
[3] M. Figueroa-Candia, F. A. Felder, and D. W. Coit, “Resiliency-based optimization of restoration policies for electric power distribution systems,” *Electric Power Systems Research*, vol. 161, pp. 188–198, 2018.
[4] A. Arif, Z. Wang, J. Wang, and C. Chen, “Power distribution system outage management with co-optimization of repairs, reconfiguration, and dg dispatch,” *IEEE Transactions on Smart Grid*, vol. 9, no. 5, pp. 4109–4118, 2017.
[5] A. Álzate, O. D. Montoya, R. A. Hincapié, and M. Granada, “Optimal location of reclosers in distribution systems considering reliability in communication channels,” in *2015 IEEE 6th Latin American Symposium on Circuits Systems (LASCAS)*, pp. 1–4, 2015.
[6] G. H. Reddy, P. Chakrapani, A. K. Goswami, and N. B. D. Choudhury, “Fuzzy based approach for restoration of distribution system during post natural disasters,” *IEEE Access*, vol. 6, pp. 3448–3458, 2017.
[7] FICO, “FICO Xpress Optimization Suite.” http://www.fico.com/en/products/, 2021. Online; accessed 29 January 2021.
[8] M. Saltos-Rodríguez, M. Aguirre-Velasco, A. Velásquez-Lozano, D. Ortiz-Villalba, and A. Villamarín-Jácome, “Distributed generation for resilience enhancement on power distribution system against lahars occurrence after a volcanic eruption,” in *2021 IEEE PES Innovative Smart Grid Technologies Conference - Latin America (ISGT Latin America)*, pp. 1–5, 2021.
[9] M. Panteli, P. Mancarella, D. N. Trakas, E. Kyriakides, and N. D. Hatziargyriou, “Metrics and quantification of operational and infrastructure resilience in power systems,” *IEEE Transactions on Power Systems*, vol. 32, no. 6, pp. 4732–4742, 2017.
[10] A. Arif, Z. Wang, C. Chen, and J. Wang, “Repair and resource scheduling in unbalanced distribution systems using neighborhood search,” *IEEE Transactions on Smart Grid*, vol. 11, no. 1, pp. 673–685, 2019.
[11] A. Zidan, H. A. Gabbar, and A. Eldessouky, “Optimal planning of combined heat and power systems within microgrids,” *Energy*, vol. 93, pp. 235–244, 2015.
[12] M. Saltos-Rodríguez, M. Aguirre-Velasco, A. Velásquez-Lozano, A. Villamarín-Jácome, J. Haro, and D. Ortiz-Villalba, “Resilience assessment in electric power systems against volcanic eruptions: Case on lahars occurrence,” in *2021 IEEE Green Technologies Conference (GreenTech)*, pp. 305–311, 2021.
[13] “IEEE PES AMPS DSAS test feeder working group avaliable: https://site.ieee.org/pes-testfeeders/resources/,” Sept. 2020.
[14] J. Jardini, C. Tahan, M. Gouvea, S. Ahn, and F. Figueiredo, “Daily load profiles for residential, commercial and industrial low voltage consumers,” *IEEE Transactions on Power Delivery*, vol. 15, no. 1, pp. 375–380, 2000.
[15] ELEPCO S.A, “ELEPCO GEOPORTAL.” https://gis-sigde.maps.arcgis.com/apps/webappviewer/index.html?id=aa01636ecf6448cf82bd2dae559a63c0, 2021. Online; accessed 29 January 2021.
[16] SNGR, “SECRETARIA NACIONAL DE GESTION DE RIESGOS.” https://www.gestionderiesgos.gob.ec/wp-contentuploads201508cotopaxi-pdf/, 2021. Online; accessed 29 January 2021.
[17] A. Velásquez-Lozano, M. Aguirre-Velasco, M. Saltos-Rodríguez, D. Ortiz-Villalba, and A. Villamarín-Jácome, “Optimal planning of var compensator for voltage regulation enhancement on power distribution systems against volcanic eruptions events,” in *2021 IEEE Green Technologies Conference (GreenTech)*, pp. 298–304, 2021.